

Crystal structure and Hirshfeld surface analysis of 2-chloro-*N*-(4-methoxyphenyl)acetamide

Mohcine Missioui,^a Walid Guerrab,^a Intissar Nchioua,^a Abderrazzak El Moutaouakil Ala Allah,^a Camille Kalonji Mubengayi,^b Abdulsalam Alsubari,^{c*} Joel T. Mage^d and Youssef Ramli^{a*}

Received 18 May 2022

Accepted 28 May 2022

Edited by L. Van Meervelt, Katholieke Universiteit Leuven, Belgium

Keywords: crystal structure; hydrogen bond; C—H··· π (ring) interaction; acetamide; Hirshfeld surface.

CCDC reference: 2175514

Supporting information: this article has supporting information at journals.iucr.org/e

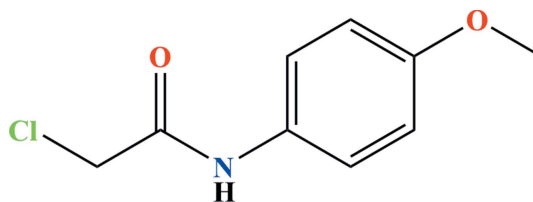
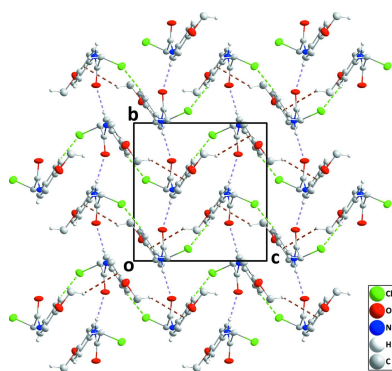
^aLaboratory of Medicinal Chemistry, Drug Sciences Research Center, Faculty of Medicine and Pharmacy, Mohammed V University in Rabat, Morocco, ^bLaboratoire de Chimie et Biochimie, Institut Supérieur des Techniques Médicales de Kinshasa, République Démocratique du Congo, ^cLaboratory of Medicinal Chemistry, Faculty of Clinical Pharmacy, 21 September University, Yemen, and ^dDepartment of Chemistry, Tulane University, New Orleans, LA 70118, USA.

*Correspondence e-mail: alsubaripharmaco@21umas.edu.ye, y.ramli@um5r.ac.ma

In the title molecule, C₉H₁₀ClNO₂, the methoxy group lies very close to the plane of the phenyl ring while the acetamido group is twisted out of this plane by 28.87 (5)°. In the crystal, a three-dimensional structure is generated by N—H···O, C—H···O and C—H···Cl hydrogen bonds plus C—H··· π (ring) interactions. A Hirshfeld surface analysis of the intermolecular interactions was performed and indicated that C···H/H···C interactions make the largest contribution to the surface area (33.4%).

1. Chemical context

Amides play a very important role in organic synthesis, including the production of medicines, functional materials, and bioactive molecules (Alcaide *et al.*, 2007; Zhang *et al.*, 2012; García-Álvarez *et al.*, 2013; Ramli & Essassi, 2015; Álvarez-Pérez *et al.*, 2019). In particular, *N*-arylacetamides are significant intermediates for the synthesis of medicinal, agrochemical, and pharmaceutical compounds (Beccalli *et al.*, 2007; Valeur & Bradley, 2009; Allen & Williams, 2011; Missioui *et al.*, 2021, 2022a,b,c). Given the wide range of therapeutic applications for such compounds, and in a continuation of our research efforts to synthesize more *N*-arylacetamides (Missioui *et al.*, 2020; Guerrab *et al.*, 2021), we report the synthesis, molecular and crystal structure and Hirshfeld surface analysis of the title compound, 2-chloro-*N*-(4-methoxyphenyl)acetamide.



2. Structural commentary

The methoxy group lies close to the mean plane of the phenyl ring C3–C8, as indicated by the C7–C6–O2–C9 torsion angle of $-174.61(10)^\circ$ and atom C9 deviating by only 0.065 (1) Å from the mean plane through the C3–C8 ring. In contrast, the acetamido group is rotated out of the above



OPEN ACCESS

Published under a CC BY 4.0 licence

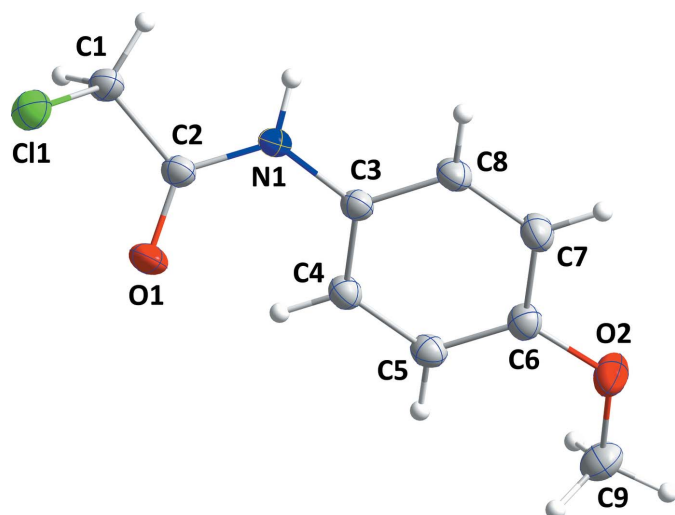


Figure 1
The molecular structure of the title molecule with labelling scheme and 50% probability ellipsoids.

plane with the dihedral angle between the mean plane through the C3–C8 ring and that defined by N1/C2/C1/O1 being 28.87 (5)° (Fig. 1). The sum of the angles about N1 is 360.0 (9)°, indicating it to be planar (sp^2 hybridization). The Cl1–C1–C2–O1 torsion angle is 52.89 (12)°, illustrating a + *synclinal* (+ *gauche*) conformation about the C1–C2 bond. This places atom Cl1 at 1.299 (1) Å from the plane defined by C1, C2, N1 and O1.

3. Supramolecular features

In the crystal, N1–H1···O1 hydrogen bonds (Table 1) form helical chains along the 2_1 axes. These chains are linked by C1–H1A···O2 hydrogen bonds (Table 1), forming layers of molecules parallel to the *ab* plane (Fig. 2). The layers are linked by weak C4–H4···Cl1 hydrogen bonds as well as by

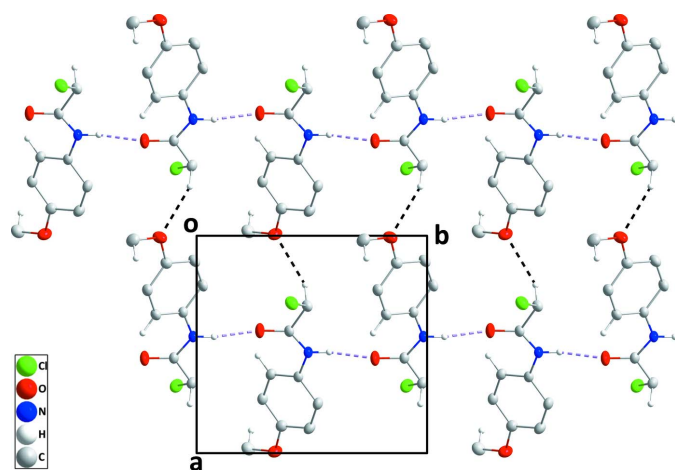


Figure 2
A portion of one layer of the crystal packing viewed along the *c*-axis direction with N–H···O and C–H···O hydrogen bonds depicted, respectively, by violet and black dashed lines. Non-interacting hydrogen atoms are omitted for clarity.

Table 1
Hydrogen-bond geometry (Å, °).

Cg1 is the centroid of the C3–C8 benzene ring.

<i>D</i> –H··· <i>A</i>	<i>D</i> –H	H··· <i>A</i>	<i>D</i> ··· <i>A</i>	<i>D</i> –H··· <i>A</i>
N1–H1···O1 ⁱ	0.89 (1)	2.01 (1)	2.8910 (11)	171 (1)
C1–H1A···O2 ⁱⁱ	0.99	2.48	3.3347 (13)	145
C4–H4···Cl1 ⁱⁱⁱ	0.95	2.83	3.7646 (10)	167
C9–H9B···Cg1 ^{iv}	0.98	2.72	3.5020 (13)	137

Symmetry codes: (i) $-x + 1, y + \frac{1}{2}, -z + \frac{3}{2}$; (ii) $x - 1, y, z$; (iii) $x, -y + \frac{1}{2}, z - \frac{1}{2}$; (iv) $x, -y - \frac{1}{2}, z - \frac{3}{2}$.

C9–H9B···Cg1 interactions (Table 1) to generate the final three-dimensional structure (Fig. 3). As the shortest distance between parallel phenyl rings is 5.1075 (7) Å, there are no π – π stacking interactions present.

4. Database survey

A search of the Cambridge Structural Database (CSD, updated to March 2022; Groom *et al.*, 2016) using the fragment **A** (Fig. 4, *R* = undefined, *X* = halogen) yielded 15 hits of which 13 had *X* = Cl and *R* = OEt (DELZIE; Zhang *et al.*, 2006), COOEt (HEGLOW; Behbehani & Ibrahim, 2012), F (JODQEZ; Kang *et al.*, 2008), S(O)₂NH(C₃HNO(CH₃)) (NULZEC; Murtaza *et al.*, 2019), SO₂NH₂ (PINXAO; Florke & Saeed, 2018; QUYRIM; Akkurt *et al.*, 2010), SME (QUGTEU; Mongkholkeaw *et al.*, 2020), H (RIYWIG; Gowda *et al.*, 2008), NO₂ (WEPGEE; Wen *et al.*, 2006; WEPGEE01;

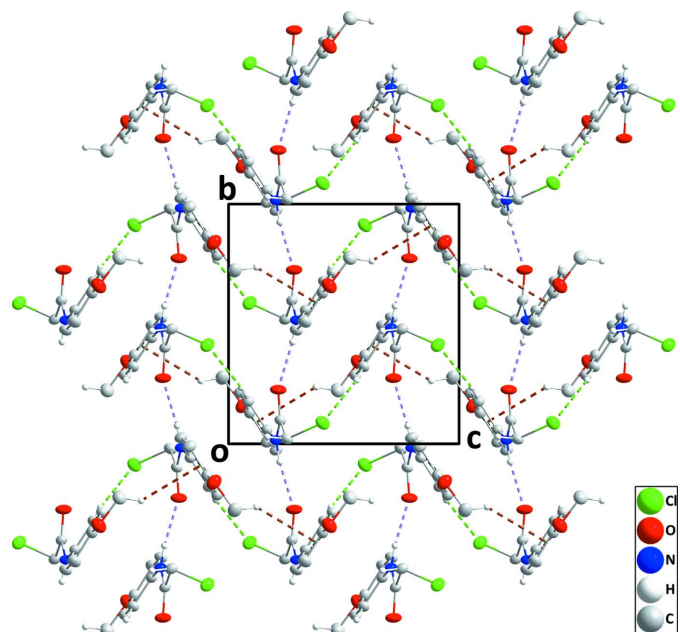


Figure 3
Packing viewed along the *a*-axis direction with N–H···O, C–H···O and C–H···Cl hydrogen bonds depicted, respectively by violet, black and light green dashed lines. C–H··· π (ring) interactions are depicted by brown dashed lines and non-interacting hydrogen atoms are omitted for clarity.

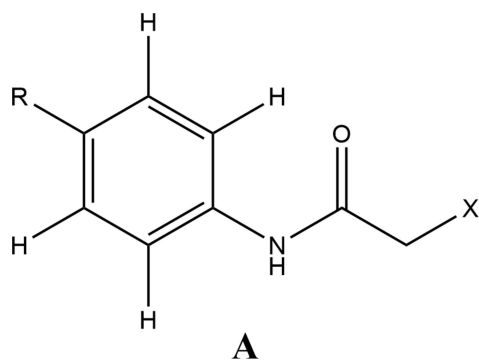


Figure 4
Fragment **A** used in the Cambridge Structural Database search.

Gowda *et al.*, 2007a), Cl (WINSUI; Gowda *et al.*, 2007b), MeC(=O) (XABWEF; Ashraf *et al.*, 2016) and Me (XICMAY; Gowda *et al.*, 2007c). The last two hits had $X = \text{Br}$ and $R = \text{Br}$ (FOWYIA; Gowda *et al.*, 2009) and $\text{CH}_2\text{CH}_2\text{O}_2\text{CC}(\text{F})(\text{SPh})(\text{NO}_2)$ (VAGCOV; Takeuchi *et al.*, 1988). In general, the conformation of the haloacetamide portion is quite similar in all structures, as is the formation of infinite chains by $\text{N}-\text{H}\cdots\text{O}$ hydrogen bonds and these are comparable to the features found in the title structure. In DELZIE and XABWEF, $\text{C}-\text{H}\cdots\pi(\text{ring})$ interactions assist in the packing, as also observed for the title molecule.

5. Hirshfeld surface analysis

The analysis was performed with *CrystalExplorer 21.5* (Spackman *et al.*, 2021) with the details of the pictorial output described in a recent publication (Tan *et al.*, 2019). Fig. 5 shows the d_{norm} surface for the asymmetric unit plotted over the range -0.5547 to 0.9665 arbitrary units together with two adjacent molecules that are part of one infinite chain and two in adjacent chains (*cf.* Fig. 2). The bright-red spots at the top and bottom indicate the $\text{N}-\text{H}\cdots\text{O}$ hydrogen bonds (blue arrows) while the fainter ones at the far right and left indicate the $\text{C}-\text{H}\cdots\text{O}$ hydrogen bonds linking the chains (curved black lines) while that below and to the right of the Cl atom represents the weak $\text{C}-\text{H}\cdots\text{Cl}$ hydrogen bonds. Fig. 6a is the fingerprint plot showing all intermolecular interactions while

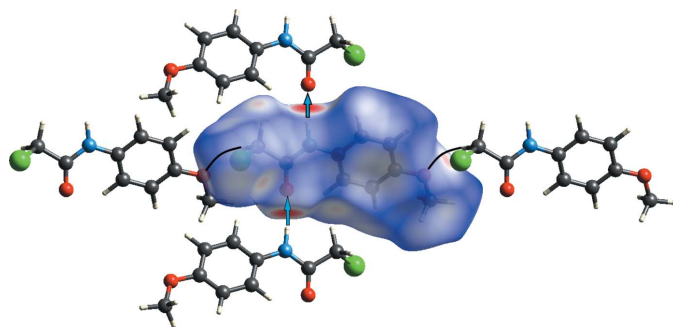


Figure 5
The Hirshfeld surface of the title molecule with two adjacent molecules involved in the $\text{N}-\text{H}\cdots\text{O}$, hydrogen bonded chain and two involving the $\text{Cl}-\text{H1A}\cdots\text{O2}$ hydrogen bonds. The former interaction is depicted by blue arrows and the latter by curved black lines.

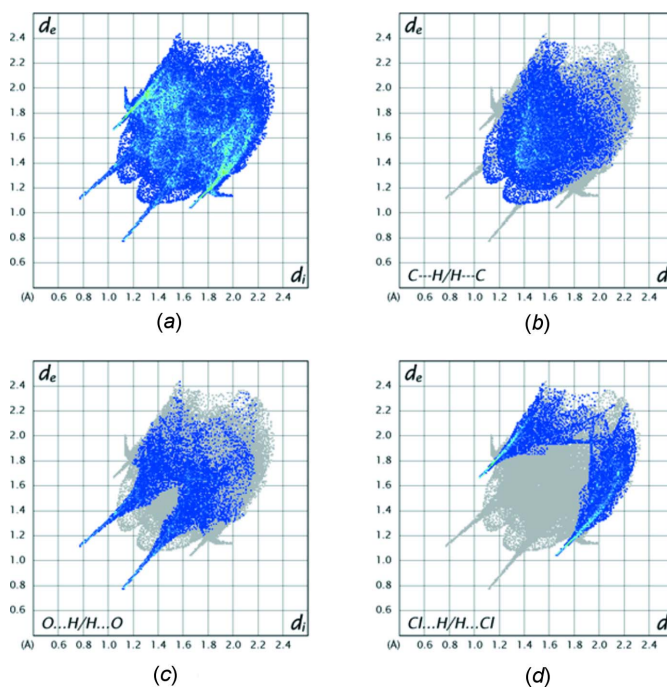


Figure 6
Fingerprint plots for the title molecule: (a), all intermolecular interactions; (b), $\text{C}\cdots\text{H}/\text{H}\cdots\text{C}$ interactions; (c), $\text{O}\cdots\text{H}/\text{H}\cdots\text{O}$ interactions; (d), $\text{Cl}\cdots\text{H}/\text{H}\cdots\text{Cl}$ interactions.

Fig. 6b–6d show these resolved into $\text{C}\cdots\text{H}/\text{H}\cdots\text{C}$ (33.4%), $\text{O}\cdots\text{H}/\text{H}\cdots\text{O}$ (19.5%) and $\text{Cl}\cdots\text{H}/\text{H}\cdots\text{Cl}$ (20%) interactions, respectively.

6. Synthesis and crystallization

0.047 mol of 4-methoxyaniline were dissolved in 40 mL of pure acetic acid and put in an ice bath. Subsequently, chloroacetyl chloride (0.047 mol) was added portionwise under stirring. At the end of the reaction, a solution of sodium acetate (35 mL) was added and a solid precipitate appeared after 30 min of stirring at room temperature. The resulting solid was filtered and washed with cold water, dried and recrystallized from ethanol to give the title compound as colourless crystals.

Yield 80%, m.p. = $398.6\text{--}400.3$ K, FT-IR (ATR, ν , cm^{-1}) 3292 (ν N–H amide), 1029 (ν N–C amide), 1660 (ν C=O amide), 3073 (ν C–H_{arom}), 827 (ν C–Cl), 2959 (ν C–H, CH₂), ¹H NMR (DMSO-*d*₆) δ ppm: 3.74 (3H, *s*, CH₃); 4.24 (2H, *s*, CH₂), 6.93–7.5 (4H, *m*, $J = 1.3$ Hz, H_{arom}), 10.23 (1H, *s*, NH), ¹³C NMR (DMSO-*d*₆) δ ppm: 43.48 (CH₂), 55.23 (CH₃), 131.53 (C_{arom}–N), 155.51 (C_{arom}–O), 113.92–120.92 (C_{arom}), 164.13 (C=O); HRMS (ESI-MS) (m/z) calculated for C₉H₁₀ClNO₂ 199.04, found 199.0105.

7. Refinement

Crystal data, data collection and structure refinement details are summarized in Table 2. Hydrogen atoms attached to carbon were placed in idealized positions and included as

Table 2

Experimental details.

Crystal data	
Chemical formula	C ₉ H ₁₀ ClNO ₂
<i>M_r</i>	199.63
Crystal system, space group	Monoclinic, <i>P2₁/c</i>
Temperature (K)	172
<i>a</i> , <i>b</i> , <i>c</i> (Å)	10.0939 (5), 9.6423 (5), 10.2799 (5)
β (°)	115.531 (2)
<i>V</i> (Å ³)	902.83 (8)
<i>Z</i>	4
Radiation type	Mo <i>K</i> α
μ (mm ⁻¹)	0.39
Crystal size (mm)	0.29 × 0.25 × 0.09
Data collection	
Diffractometer	Bruker D8 QUEST PHOTON 3 diffractometer
Absorption correction	Numerical (<i>SADABS</i> ; Krause <i>et al.</i> , 2015)
<i>T_{min}</i> , <i>T_{max}</i>	0.91, 0.97
No. of measured, independent and observed [<i>I</i> > 2 σ (<i>I</i>)] reflections	43210, 2871, 2508
<i>R_{int}</i>	0.034
($\sin \theta/\lambda$) _{max} (Å ⁻¹)	0.726
Refinement	
<i>R</i> [<i>F</i> ² > 2 σ (<i>F</i> ²)], <i>wR</i> (<i>F</i> ²), <i>S</i>	0.032, 0.091, 1.10
No. of reflections	2871
No. of parameters	123
No. of restraints	1
H-atom treatment	H atoms treated by a mixture of independent and constrained refinement
$\Delta\rho_{\max}$, $\Delta\rho_{\min}$ (e Å ⁻³)	0.38, -0.21

Computer programs: *APEX3* and *SAINT* (Bruker, 2020), *SHELXT* (Sheldrick, 2015a), *SHELXL2018/1* (Sheldrick, 2015b), *DIAMOND* (Brandenburg & Putz, 2012) and *SHELXTL* (Sheldrick, 2008).

riding contributions with isotropic displacement parameters fixed at 1.2*U*_{eq}(C) (1.5 for the methyl group). The N-bound H atom was found in a difference-Fourier map and refined with a DFIX 0.91 0.01 instruction and an independent isotropic displacement parameter.

Acknowledgements

JTM thanks Tulane University for support of the Tulane Crystallography Laboratory. Author contributions are as follows: conceptualization, YR; methodology, WG and CKM; investigation, IN, AEMAA and MM; theoretical calculations, JTM; writing (original draft), JTM and YR; writing (review and editing of the manuscript), YR; formal analysis, AA and MM; supervision, YR; crystal-structure determination and validation, JTM.

References

Akkurt, M., Yalçın, Ş. P., Türkmen, H. & Büyükgüngör, O. (2010). *Acta Cryst.* **E66**, o1596.
 Alcaide, B., Almendros, P. & Aragoncillo, C. (2007). *Chem. Rev.* **107**, 4437–4492.
 Allen, C. L. & Williams, J. M. J. (2011). *Chem. Soc. Rev.* **40**, 3405.
 Álvarez-Pérez, A., Esteruelas, M. A., Izquierdo, S., Varela, J. A. & Saá, C. (2019). *Org. Lett.* **21**, 5346–5350.

Ashraf, Z., Kim, D., Seo, S.-Y. & Kang, S. K. (2016). *Acta Cryst.* **C72**, 94–98.
 Beccalli, E. M., Brogini, G., Martinelli, M. & Sottocornola, S. (2007). *Chem. Rev.* **107**, 5318–5365.
 Behbehani, H. & Ibrahim, H. M. (2012). *Molecules*, **17**, 6362–6385.
 Brandenburg, K. & Putz, H. (2012). *DIAMOND*. Crystal Impact GbR, Bonn, Germany.
 Bruker (2020). *APEX3* and *SAINT*. Bruker AXS LLC, Madison, Wisconsin, USA.
 Florke, U. & Saeed, A. (2018). Private Communication (refcode PINXAO). CCDC, Cambridge, England.
 García-Álvarez, R., Crochet, P. & Cadierno, V. (2013). *Green Chem.* **15**, 46–66.
 Gowda, B. T., Foro, S. & Fuess, H. (2007a). *Acta Cryst.* **E63**, o2335–o2336.
 Gowda, B. T., Foro, S. & Fuess, H. (2007b). *Acta Cryst.* **E63**, o4488.
 Gowda, B. T., Foro, S. & Fuess, H. (2007c). *Acta Cryst.* **E63**, o2333–o2334.
 Gowda, B. T., Kožíšek, J., Tokarčík, M. & Fuess, H. (2008). *Acta Cryst.* **E64**, o987.
 Gowda, B. T., Svoboda, I., Foro, S., Suchetan, P. A. & Fuess, H. (2009). *Acta Cryst.* **E65**, o1955.
 Groom, C. R., Bruno, I. J., Lightfoot, M. P. & Ward, S. C. (2016). *Acta Cryst.* **B72**, 171–179.
 Guerrab, W., Missioui, M., Zaoui, Y., Mague, J. T. & Ramli, Y. (2021). *Z. Kristallogr. New Cryst. Struct.* **236**, 133–134.
 Kang, S., Zeng, H., Li, H. & Wang, H. (2008). *Acta Cryst.* **E64**, o1194.
 Krause, L., Herbst-Irmer, R., Sheldrick, G. M. & Stalke, D. (2015). *J. Appl. Cryst.* **48**, 3–10.
 Missioui, M., Guerrab, W., Mague, J. T. & Ramli, Y. (2020). *Z. Kristallogr. New Cryst. Struct.* **235**, 1429–1430.
 Missioui, M., Lgaz, H., Guerrab, W., Lee, H., Warad, I., Mague, J. T., Ali, I. H., Essassi, E. M. & Ramli, Y. (2022a). *J. Mol. Struct.* **1253**, 132132.
 Missioui, M., Mortada, S., Guerrab, W., Serdaroglu, G., Kaya, S., Mague, J. T., Essassi, E. M., Faouzi, M. E. A. & Ramli, Y. (2021). *J. Mol. Struct.* **1239**, 130484.
 Missioui, M., Said, M. A., Demirtaş, G., Mague, J. T., Al-Sulami, A., Al-Kaff, N. S. & Ramli, Y. (2022b). *Arab. J. Chem.* **15**, 103595.
 Missioui, M., Said, M. A., Demirtaş, G., Mague, J. T. & Ramli, Y. (2022c). *J. Mol. Struct.* **1247**, 131420.
 Mongkholkeaw, S., Songsasen, A., Duangthongyou, T., Chainok, K., Suramit, S., Wattanathana, W. & Wannalarse, B. (2020). *Acta Cryst.* **E76**, 594–598.
 Murtaza, S., Altaf, A. A., Hamayun, M., Iftikhar, K., Tahir, M. N., Tariq, J. & Faiz, K. (2019). *Eur. J. Chem.* **10**, 358–366.
 Ramli, Y. & Essassi, E. M. (2015). *Adv. Chem. Res.* **27**, 109–160.
 Sheldrick, G. M. (2008). *Acta Cryst.* **A64**, 112–122.
 Sheldrick, G. M. (2015a). *Acta Cryst.* **A71**, 3–8.
 Sheldrick, G. M. (2015b). *Acta Cryst.* **C71**, 3–8.
 Spackman, P. R., Turner, M. J., McKinnon, J. J., Wolff, S. K., Grimwood, D. J., Jayatilaka, D. & Spackman, M. A. (2021). *J. Appl. Cryst.* **54**, 1006–1011.
 Takeuchi, Y., Nojiri, M., Koizumi, T. & Iitaka, Y. (1988). *Tetrahedron Lett.* **29**, 4727–4730.
 Tan, S. L., Jotani, M. M. & Tiekink, E. R. T. (2019). *Acta Cryst.* **E75**, 308–318.
 Valeur, E. & Bradley, M. (2009). *Chem. Soc. Rev.* **38**, 606–631.
 Wen, Y.-H., Li, X.-M., Xu, L.-L., Tang, X.-F. & Zhang, S.-S. (2006). *Acta Cryst.* **E62**, o4427–o4428.
 Zhang, D., Zhao, X., Hou, J. & Li, Z. (2012). *Chem. Rev.* **112**, 5271–5316.
 Zhang, S.-S., Wen, H.-L., Li, X.-M., Xu, L.-L. & Wen, Y.-H. (2006). *Acta Cryst.* **E62**, o3412–o3413.

supporting information

Acta Cryst. (2022). E78, 687-690 [https://doi.org/10.1107/S205698902200576X]

Crystal structure and Hirshfeld surface analysis of 2-chloro-*N*-(4-methoxyphenyl)acetamide

Mohcine Missioui, Walid Guerrab, Intissar Nchioua, Abderrazzak El Moutaouakil Ala Allah, Camille Kalonji Mubengayi, Abdulsalam Alsubari, Joel T. Mague and Youssef Ramli

Computing details

Data collection: *APEX3* (Bruker, 2020); cell refinement: *SAINTE* (Bruker, 2020); data reduction: *SAINTE* (Bruker, 2020); program(s) used to solve structure: *SHELXT* (Sheldrick, 2015*a*); program(s) used to refine structure: *SHELXL2018/1* (Sheldrick, 2015*b*); molecular graphics: *DIAMOND* (Brandenburg & Putz, 2012); software used to prepare material for publication: *SHELXTL* (Sheldrick, 2008).

2-Chloro-*N*-(4-methoxyphenyl)acetamide

Crystal data

C₉H₁₀ClNO₂

$M_r = 199.63$

Monoclinic, *P*2₁/*c*

$a = 10.0939$ (5) Å

$b = 9.6423$ (5) Å

$c = 10.2799$ (5) Å

$\beta = 115.531$ (2)°

$V = 902.83$ (8) Å³

$Z = 4$

$F(000) = 416$

$D_x = 1.469$ Mg m⁻³

Mo *K* α radiation, $\lambda = 0.71073$ Å

Cell parameters from 9903 reflections

$\theta = 2.2\text{--}31.1^\circ$

$\mu = 0.39$ mm⁻¹

$T = 172$ K

Plate, colourless

0.29 × 0.25 × 0.09 mm

Data collection

Bruker D8 QUEST PHOTON 3
diffractometer

Radiation source: fine-focus sealed tube

Graphite monochromator

Detector resolution: 7.3910 pixels mm⁻¹

φ and ω scans

Absorption correction: numerical
(*SADABS*; Krause *et al.*, 2015)

$T_{\min} = 0.91$, $T_{\max} = 0.97$

43210 measured reflections

2871 independent reflections

2508 reflections with $I > 2\sigma(I)$

$R_{\text{int}} = 0.034$

$\theta_{\max} = 31.1^\circ$, $\theta_{\min} = 3.1^\circ$

$h = -14 \rightarrow 14$

$k = -13 \rightarrow 13$

$l = -14 \rightarrow 14$

Refinement

Refinement on F^2

Least-squares matrix: full

$R[F^2 > 2\sigma(F^2)] = 0.032$

$wR(F^2) = 0.091$

$S = 1.10$

2871 reflections

123 parameters

1 restraint

Primary atom site location: dual

Secondary atom site location: difference Fourier
map

Hydrogen site location: mixed

H atoms treated by a mixture of independent
and constrained refinement

$w = 1/[\sigma^2(F_o^2) + (0.0462P)^2 + 0.2203P]$

where $P = (F_o^2 + 2F_c^2)/3$

$$(\Delta/\sigma)_{\max} = 0.001$$

$$\Delta\rho_{\max} = 0.38 \text{ e } \text{\AA}^{-3}$$

$$\Delta\rho_{\min} = -0.21 \text{ e } \text{\AA}^{-3}$$

Special details

Experimental. The diffraction data were obtained from 7 sets of frames, each of width 0.5° in ω or φ , collected with scan parameters determined by the "strategy" routine in *APEX3*. The scan time was 6 sec/frame.

Geometry. All esds (except the esd in the dihedral angle between two l.s. planes) are estimated using the full covariance matrix. The cell esds are taken into account individually in the estimation of esds in distances, angles and torsion angles; correlations between esds in cell parameters are only used when they are defined by crystal symmetry. An approximate (isotropic) treatment of cell esds is used for estimating esds involving l.s. planes.

Refinement. Refinement of F^2 against ALL reflections. The weighted R-factor wR and goodness of fit S are based on F^2 , conventional R-factors R are based on F, with F set to zero for negative F^2 . The threshold expression of $F^2 > 2\sigma(F^2)$ is used only for calculating R-factors(gt) etc. and is not relevant to the choice of reflections for refinement. R-factors based on F^2 are statistically about twice as large as those based on F, and R-factors based on ALL data will be even larger. H-atoms attached to carbon were placed in calculated positions (C—H = 0.95 - 0.99 Å) and were included as riding contributions with isotropic displacement parameters 1.2 - 1.5 times those of the attached atoms. That attached to nitrogen was placed in a location derived from a difference map and refined with a DFIX 0.91 0.01 instruction.

Fractional atomic coordinates and isotropic or equivalent isotropic displacement parameters (\AA^2)

	x	y	z	$U_{\text{iso}}^*/U_{\text{eq}}$
Cl1	0.30989 (3)	0.41222 (3)	0.90827 (3)	0.03169 (9)
O1	0.43630 (10)	0.27410 (8)	0.71560 (10)	0.03148 (19)
O2	0.99240 (9)	0.34016 (9)	0.56309 (9)	0.03316 (19)
N1	0.53618 (9)	0.48405 (8)	0.70583 (9)	0.02160 (17)
H1	0.5353 (17)	0.5749 (9)	0.7222 (16)	0.034 (4)*
C1	0.32272 (11)	0.47958 (10)	0.75260 (11)	0.02423 (19)
H1A	0.226444	0.470886	0.667909	0.029*
H1B	0.348725	0.579198	0.767150	0.029*
C2	0.43834 (11)	0.40146 (10)	0.72459 (10)	0.02147 (19)
C3	0.64850 (11)	0.44121 (10)	0.66649 (10)	0.02036 (18)
C4	0.63724 (11)	0.32251 (10)	0.58566 (11)	0.02264 (19)
H4	0.552126	0.265906	0.555512	0.027*
C5	0.75029 (11)	0.28609 (10)	0.54860 (10)	0.02332 (19)
H5	0.742024	0.204773	0.493437	0.028*
C6	0.87484 (11)	0.36845 (11)	0.59218 (11)	0.02389 (19)
C7	0.88452 (12)	0.48995 (11)	0.66987 (12)	0.0275 (2)
H7	0.968462	0.547843	0.697712	0.033*
C8	0.77218 (12)	0.52620 (10)	0.70637 (11)	0.0249 (2)
H8	0.779097	0.609174	0.758744	0.030*
C9	0.97987 (13)	0.22369 (13)	0.47330 (13)	0.0325 (2)
H9A	1.070019	0.214361	0.460154	0.049*
H9B	0.896160	0.237045	0.379304	0.049*
H9C	0.964803	0.139514	0.518658	0.049*

Atomic displacement parameters (\AA^2)

	U^{11}	U^{22}	U^{33}	U^{12}	U^{13}	U^{23}
Cl1	0.03574 (16)	0.03273 (15)	0.03447 (15)	0.00576 (10)	0.02258 (12)	0.00686 (10)
O1	0.0429 (5)	0.0163 (3)	0.0466 (5)	-0.0005 (3)	0.0300 (4)	0.0011 (3)

O2	0.0278 (4)	0.0390 (5)	0.0389 (4)	-0.0049 (3)	0.0202 (3)	-0.0107 (3)
N1	0.0247 (4)	0.0154 (4)	0.0269 (4)	-0.0001 (3)	0.0133 (3)	-0.0006 (3)
C1	0.0259 (5)	0.0214 (4)	0.0278 (5)	0.0031 (3)	0.0139 (4)	0.0043 (4)
C2	0.0253 (4)	0.0181 (4)	0.0226 (4)	0.0010 (3)	0.0118 (4)	0.0022 (3)
C3	0.0228 (4)	0.0177 (4)	0.0213 (4)	0.0002 (3)	0.0102 (3)	0.0013 (3)
C4	0.0239 (4)	0.0204 (4)	0.0240 (4)	-0.0033 (3)	0.0107 (3)	-0.0022 (3)
C5	0.0275 (5)	0.0206 (4)	0.0232 (4)	-0.0013 (3)	0.0121 (4)	-0.0027 (3)
C6	0.0252 (4)	0.0255 (5)	0.0229 (4)	-0.0010 (4)	0.0122 (4)	-0.0002 (3)
C7	0.0278 (5)	0.0256 (5)	0.0320 (5)	-0.0071 (4)	0.0156 (4)	-0.0051 (4)
C8	0.0286 (5)	0.0194 (4)	0.0283 (5)	-0.0041 (4)	0.0139 (4)	-0.0042 (3)
C9	0.0336 (6)	0.0345 (6)	0.0336 (6)	0.0051 (4)	0.0184 (5)	-0.0027 (4)

Geometric parameters (Å, °)

C11—C1	1.7828 (10)	C4—C5	1.3947 (14)
O1—C2	1.2310 (12)	C4—H4	0.9500
O2—C6	1.3704 (13)	C5—C6	1.3880 (14)
O2—C9	1.4243 (14)	C5—H5	0.9500
N1—C2	1.3457 (13)	C6—C7	1.3973 (15)
N1—C3	1.4194 (13)	C7—C8	1.3840 (15)
N1—H1	0.893 (9)	C7—H7	0.9500
C1—C2	1.5172 (14)	C8—H8	0.9500
C1—H1A	0.9900	C9—H9A	0.9800
C1—H1B	0.9900	C9—H9B	0.9800
C3—C4	1.3900 (13)	C9—H9C	0.9800
C3—C8	1.3989 (14)		
C6—O2—C9	117.06 (9)	C6—C5—C4	120.11 (9)
C2—N1—C3	126.46 (8)	C6—C5—H5	119.9
C2—N1—H1	119.0 (10)	C4—C5—H5	119.9
C3—N1—H1	114.5 (10)	O2—C6—C5	124.39 (9)
C2—C1—C11	110.42 (7)	O2—C6—C7	115.96 (9)
C2—C1—H1A	109.6	C5—C6—C7	119.65 (9)
C11—C1—H1A	109.6	C8—C7—C6	120.20 (9)
C2—C1—H1B	109.6	C8—C7—H7	119.9
C11—C1—H1B	109.6	C6—C7—H7	119.9
H1A—C1—H1B	108.1	C7—C8—C3	120.30 (9)
O1—C2—N1	124.69 (9)	C7—C8—H8	119.8
O1—C2—C1	121.35 (9)	C3—C8—H8	119.8
N1—C2—C1	113.91 (8)	O2—C9—H9A	109.5
C4—C3—C8	119.36 (9)	O2—C9—H9B	109.5
C4—C3—N1	122.71 (9)	H9A—C9—H9B	109.5
C8—C3—N1	117.88 (9)	O2—C9—H9C	109.5
C3—C4—C5	120.33 (9)	H9A—C9—H9C	109.5
C3—C4—H4	119.8	H9B—C9—H9C	109.5
C5—C4—H4	119.8		
C3—N1—C2—O1	3.07 (17)	C9—O2—C6—C5	4.72 (16)

C3—N1—C2—C1	-174.47 (9)	C9—O2—C6—C7	-174.61 (10)
C11—C1—C2—O1	52.89 (12)	C4—C5—C6—O2	178.93 (10)
C11—C1—C2—N1	-129.47 (8)	C4—C5—C6—C7	-1.77 (15)
C2—N1—C3—C4	27.78 (15)	O2—C6—C7—C8	-179.00 (10)
C2—N1—C3—C8	-154.97 (10)	C5—C6—C7—C8	1.64 (16)
C8—C3—C4—C5	2.04 (15)	C6—C7—C8—C3	0.34 (16)
N1—C3—C4—C5	179.25 (9)	C4—C3—C8—C7	-2.17 (15)
C3—C4—C5—C6	-0.08 (15)	N1—C3—C8—C7	-179.52 (9)

Hydrogen-bond geometry (\AA , $^\circ$)

*Cg*1 is the centroid of the C3–C8 benzene ring.

<i>D</i> —H \cdots <i>A</i>	<i>D</i> —H	H \cdots <i>A</i>	<i>D</i> \cdots <i>A</i>	<i>D</i> —H \cdots <i>A</i>
N1—H1 \cdots O1 ⁱ	0.89 (1)	2.01 (1)	2.8910 (11)	171 (1)
C1—H1 <i>A</i> \cdots O2 ⁱⁱ	0.99	2.48	3.3347 (13)	145
C4—H4 \cdots C11 ⁱⁱⁱ	0.95	2.83	3.7646 (10)	167
C9—H9 <i>B</i> \cdots <i>Cg</i> 1 ^{iv}	0.98	2.72	3.5020 (13)	137

Symmetry codes: (i) $-x+1, y+1/2, -z+3/2$; (ii) $x-1, y, z$; (iii) $x, -y+1/2, z-1/2$; (iv) $x, -y-1/2, z-3/2$.